Volume Change of Glassy Polymers by Sorption of Small Molecules and Its Relation to the Intermolecular Space

P. Gotthardt, A. Grüger, H. G. Brion, R. Plaetschke,† and R. Kirchheim*

Institut für Metallphysik, Universität Göttingen, Hospitalstrasse 3-7, D-37073 Göttingen, Germany

Received June 10, 1997; Revised Manuscript Received September 26, 1997[⊗]

ABSTRACT: The volume changes caused by the sorption of H_2O, Ar, N_2, CO_2, CH_4 and Acetone in Bisphenol-A polycarbonate and of CO_2 in different substituted polycarbonates and in Kapton were measured in a dilatometer at room temperature. The partial molar volumes of the small molecules are much smaller than the ones obtained in the liquid or rubbery state of polymers. It is a special feature of the glassy state that the partial molar volume increases as concentration increases. Both findings are explained by a model developed recently, where the volume of the site occupied by small molecules is related via elastic distortions to the solution energy into this site. Assuming a spherical shape of site volumes and a Gaussian distribution of the volumes yields an average value of 33 to 38 Å^3/site and a width of about 10 Å^3. These quantities vary in a systematic manner with the glass transition temperature and the nature of side groups of the polymer. The results are compared with values calculated from life times of o-positronium and values of the d-spacings from X-ray.

1. Introduction

The free volume of glassy polymers is often defined as the difference between the actual volume below the glass transition temperature T_g and the volume extrapolated from the linear temperature dependence above T_g.[1] Besides its ability to incorporate small molecules, it is also considered to play a major role during plastic deformation. Thus a decrease of toughness during physical aging of polymers is related to a loss of free volume.[2] Unlike the crystalline state, where diffraction methods yield lattice parameters and allow the calculation of interatomic (intermolecular) space from the known volume of atoms (molecules), the amorphous state and its free volume cannot be characterized this way. Alternative ways are to simulate the amorphous structure on a computer[3−5] or to use probes like positrons[6−8] or small molecules.[9]

Dissolving small molecules in glassy polymers gives rise to a volume increase per molecule that is smaller than the corresponding increase for the liquid or rubbery polymer. This is explained by the ability of the liquid and rubbery polymer to form anew that part of the free volume which was occupied by small molecules.[9] Thus the difference of the partial molar volumes in the glassy and liquid state is a measure of the intermolecular space. To calculate this space and its distribution, a model has been developed that relates the free volume at a given site to the dissolution energy into this site. For molecules having a volume V_g larger than the site volume V_h the polymer has to be expanded. This gives rise to an elastic distortion energy. In order to calculate this energy, a continuum analogy has been adopted, where an elastic sphere is pressed into a spherical hole of an elastic matrix. Then the matrix and the sphere are strained and the corresponding elastic energy is given by[10]

$$G_{el} = \begin{cases} \frac{2\mu_s}{3\gamma'} \frac{(V_g - V_h)^2}{V_h} & \text{for } V_g \geq V_h \\ 0 & \text{for } V_g < V_h \end{cases} \quad (1)$$

where μ_s is the shear modulus of the polymer and $\gamma' = (1 + 4\mu_s/3\kappa^*)$ is a dimensionless factor that depends on the bulk modulus κ^* of the elastic sphere. For κ^* being the same as the bulk modulus of the matrix and Poisson's ratio being $\nu = 1/3$ we obtain $\gamma' = 1.5$. In the previous paper[9] γ' did not appear in eq 1 because the molecule was assumed to be stiff, i.e. $\kappa^* \to \infty$ and $\gamma' \to 1$. However, we assume in the following that the small molecules have similar bulk moduli compared to the polymer. This may be justified by comparing bulk moduli of liquids composed of small molecules that are about 1 GPa, with those of glassy polymers being about 3 GPa. The overall volume change or the partial molar volume V_p for this case is[10]

$$V_p = \begin{cases} V_g - V_h & \text{for } V_g \geq V_h \\ 0 & \text{for } V_g < V_h \end{cases} \quad (2)$$

In general, we cannot exclude that the second line in eqs 1 and 2 are different from zero, if strong interactions between very small molecules and large holes lead to a contraction of the polymer. However, no volume contraction during sorption of small molecules has been observed so far.

Because of eq 1 a distribution of site volumes $n(V_h)$ gives rise to a distribution of site energies $n(G)$. In equilibrium the thermal occupancy of the various sites is determined by Fermi−Dirac statistics, if one site can be occupied by one molecule only. Thus the overall volume change is given by integration over all occupied sites[9]

$$\Delta V = \int_{-\infty}^{\infty} (V_g - V_h) \frac{n(G)\, dG}{1 + \exp[(G - \mu)/kT]} \quad (3)$$

where μ is the chemical potential of the small molecules. It is related to the partial pressure p of the small molecules by the well-known equation

$$\mu = \mu^\circ + kT \ln p/p_0 \quad (4)$$

with μ° being the standard value for $p = p_0 = 1$ bar. The total concentration c of dissolved small molecules is given by[11]

$$c = \int_{-\infty}^{\infty} \frac{n(G)\, dG}{1 + \exp[(G - \mu)/kT]} \quad (5)$$

† Bayer AG, Leverkusen, Germany.

⊗ Abstract published in *Advance ACS Abstracts,* November 15, 1997.

S0024-9297(97)00825-5 CCC: $14.00

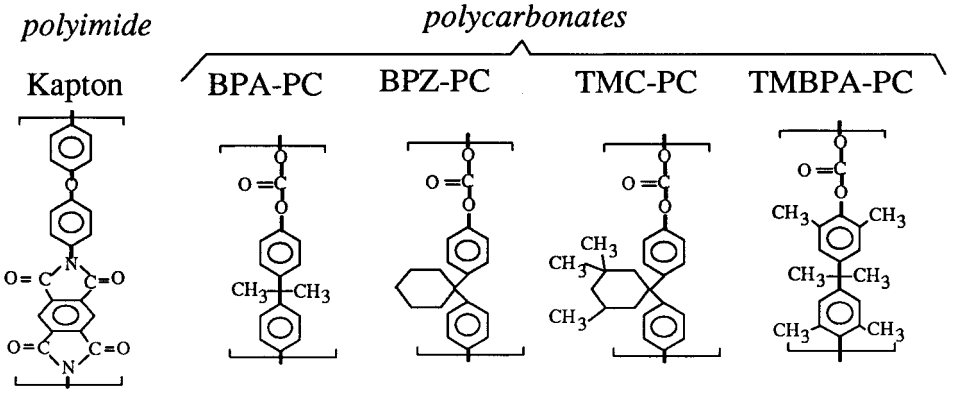

Figure 1. Structure and synonyms of the polymers used in this study. The polyimide is pyromellitic dianhydride oxydianiline (Kapton-H). The polycarbonates are on Bisphenol A basis (BPA) with substitutions between the phenyl rings, dimethyl (BPA-PC), cyclohexane (BPZ-PC), 3,3,5-trimethylcyclohexane-1 (TMC-PC), and substitutions at the phenyl ring: 3,3′,5,5′-tetramethyl-1 (TMBPA-PC).

The concept of having sites or holes for small particles in an amorphous polymer is supported by computer simulations[5] showing that loci of energy minima for small particles are separated by energy maxima. Concentration in this work is defined as the number ratio of small molecules and sites. In order to convert this into measurable quantities like cm^3 gas/cm^3 polymer, the total number of sites in a polymer has to be known (it was estimated to be 6×10^{21} cm^{-3},[11] which corresponds to 250 cm^3 gas/cm^3 polymer for total occupancy).

The choice of an appropriate distribution function $n(G)$ is more difficult, because the measured relationship between c and p is rather insensitive to it; i.e., there are always enough fitting parameters to describe $p-c$ isotherms.[11] In refs 9 and 11 the calculation of $n(G)$ is based on a Gaussian distribution for V_h. According to Bueche[12] we use

$$n(V_h) = \frac{1}{\sigma_V\sqrt{\pi}} \exp\left[-\frac{(V_h - V_h^\circ)^2}{\sigma_V^2}\right] \quad \text{with}$$

$$\sigma_V = \sqrt{\frac{2kT_gV_h^\circ}{B}} \quad (6)$$

where σ_V is the width of the distribution and V_h° its average value, T_g is the glass transition temperature of the polymer, and B is its bulk modulus at $T = T_g$. This represents the statistical fluctuation of a small volume in the liquid state being embedded in a heat bath at the glass transition temperature. Below T_g this distribution shall not change with temperature any more. By using a linear expansion of eq 1 it can be shown[11] that the site energy distribution becomes Gaussian, too, with the following first and second moments:

$$G^\circ = G_r + \frac{2\mu_s}{3\gamma'}\frac{(V_g - V_h^\circ)^2}{V_h^\circ} \quad \text{and}$$

$$\sigma_G = \frac{2\mu_s}{3\gamma'}\frac{V_g^2 - V_h^{\circ 2}}{V_h^{\circ 2}} \quad (7)$$

where G_r is a residual free energy that does not depend on site volume V_h. This way the width of the distribution could be calculated from known data of the gas and the polymer with a predictability better than 30%.

This concept was applied in ref 9 to analyze the few number of available data on volume expansion caused by small molecules. It is the main purpose of the present work to add further experimental data for a variety of small molecules (H_2O, Ar, N_2, CO_2, CH_4, and acetone) in Bisphenol A polycarbonate and of CO_2 in various substituted polycarbonates and in Kapton. Measured data and their dependence on V_g will be compared with the predictions of the model. As described in ref 9, $p-c$ isotherms were used to evaluate the parameters of the Gaussian energy distribution. The latter are inserted in eq 3 to calculate the volume change ΔV as a function of p or c. Then only one parameter V_h° is left to fit measured ΔV vs p curves by calculated ones. If a different molecule is used and if its molar volume V_g is known, no fitting parameter will be left.

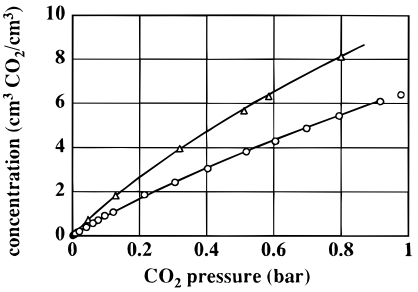

Figure 2. Pressure−concentration isotherms for CO_2 in TMC-PC at 21 (triangles) and 35 °C (circles).[13]

The results obtained for the different polymers of this study will be compared with values determined from positron annihilation studies and with d spacings of the polymers as measured by us using X-ray diffraction.

2. Experimental Section

2.1. Polymers. A Kapton H film (25 μm thick) and a Bisphenol A polycarbonate film (80 μm thick) were purchased from Goodfellow Ltd., Cambridge, U.K., and four different Bisphenol A polycarbonates with structures as shown in Figure 1 were provided by the Bayer Co. as films of about 100 μm thickness. The latter four films were produced by the Bayer Co. from solutions in methylene chloride and annealed for 4 h at 120 °C in air to remove residual solute molecules.

Sorption isotherms were determined at 21 ± 1 °C by having the polymer in a vacuum chamber filled with gas or vapor of the small molecules. By either weighing the samples or monitoring the pressure drop within the chamber, the amount of absorbed solute could be determined. The $p-c$ isotherms achieved this way were fitted to eqs 4 and 5 with the two parameters $G^\circ-\mu^\circ$ and σ_G. An example is shown in Figure 2 and experimental details are described elsewhere.[13]

With the aid of X-ray diffraction the amorphous halo of the various polymers was determined as shown for

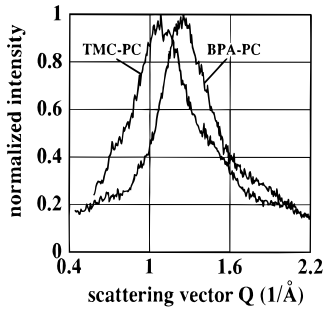

Figure 3. X-ray diffraction peak of BPA-PC and TMC-PC.

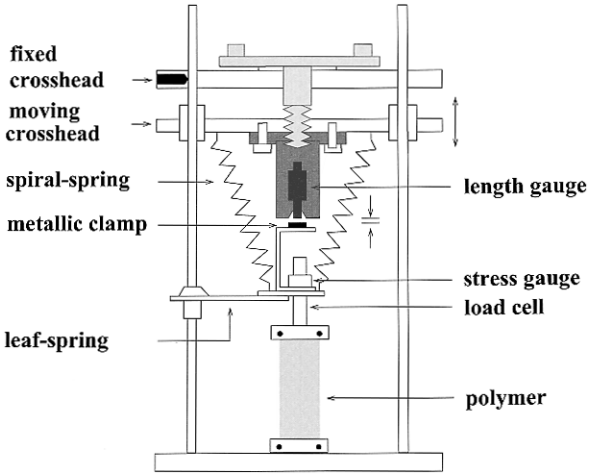

Figure 4. Schematic drawing of dilatometer 1.

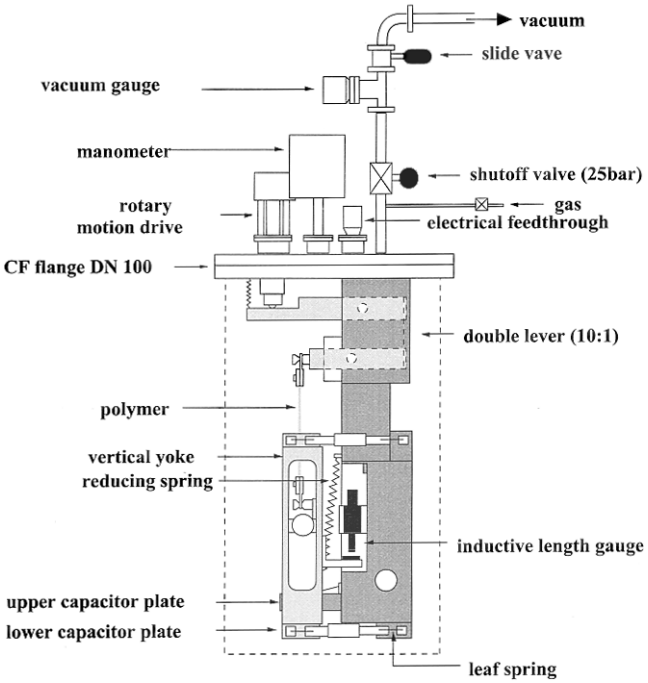

Figure 5. Schematic drawing of dilatometer 2.

two polymers in Figure 3. The scattering vector at maximum Q_m is a measure of the most frequent distance of scatterers. This distance will be called the *d* spacing ($=2\pi/Q_m$). For Kapton the peak was not as structureless as those shown in Figure 3, indicating some ordering.

2.2. Dilatometer. We build two dilatometers, which are shown in Figures 4 and 5. The first and simple one was constructed for pressures below 1 bar within a rather large vacuum chamber of about 50 L. The polymer film (about 2 cm width and 10 cm length) was clamped at two ends and stretched by two spiral springs. The applied tensile stress as measured by a stress gauge was much below the yield strength. During evacuation of the chamber to a base pressure of 10^{-5} mbar, residual gasses were removed from the sample. Gases or vapors were introduced into the chamber through a valve until a given pressure was reached. Pressures were always measured by capacitance manometers. Changes of sample length were monitored with a commercially available length gauge (I-W-A A4, Dornier, Friedrichshafen, Germany) based on inductance changes occurring during the approach of the free moving metallic clamp at one end of the film (cf. Figure 4). Thus, by assuming isotropic dilatation, volume changes could be measured *in situ* during sorption of small molecules. Extrapolating a small linear drift back to $t = 0$, where the sample was exposed to the gas (cf. section 2.3), the total length change Δl was obtained and related to the corresponding volume change ΔV by $3\Delta l/l_0 = \Delta V/V_0$ with l_0 and V_0 being the initial length or volume of the sample. Measurements were made in an environment of constant temperature (21 ± 1 °C). The drawbacks of this low-pressure dilatometer were the following: (1) limitation in the upper pressure, which makes it unsuitable for gases of low solubility, (2) large volume, which does not allow measuring the amount of absorbed gas from a pressure drop, (3) difficult temperature control due to a large volume of the chamber, and (4) a rather pronounced drift of the length gauge, excluding measurements with gases of low solubility and slow diffusivity (long time experiments).

In order to avoid all these disadvantages a second compact dilatometer was built as shown in Figure 5. Again the film of about 2 cm width and 8 cm length is mounted between two clamps. The lower clamp is attached to the upper condenser plate of the capacitance length gauge, and a metal plate is used for the inductive length gauge. The latter was installed in addition because it is more sensitive at larger length changes. The capacitance plates are shielded by concentric rings and the measurement of the capacitance was conducted as described in ref 14 with the aid of a capacitance bridge (HP4280/1 MHz). The sample is strechted by the weight of the lower clamp and the other metal pieces attached to it. In order to avoid excessive tensile stresses in the sample, the weight of the lower clamp can be reduced by an adjustable spring. In addition, four leaf springs do not allow a larger horizontal movement of the lower clamp and prohibit tilting of the capacitor plates. The upper clamp can be moved via a feed through and a double cantilever from outside the vacuum chamber. This way the lower clamp is moved as well, in order to bring the lower condenser plate into a favorable position. The inductive length gauge was used to calibrate the capacitance gauge. The latter had a sensitivity of 3−60 nm for length changes between $\Delta l = 0$ and 100 μm. Above 100 μm the short time detection limit of the inductive gauge was smaller and independent of the total length change Δl. Temperature control was achieved by inserting the vacuum chamber into a water bath of controlled temperature. The same bath was used for the copper pipes connecting the gas supply and gas valve to avoid a temperature difference between the gas and sample. The temperature sensitivity of this dilatometer is 1 μm/K.

The unoccupied volume within the vacuum chamber is now 1250 cm^3. Besides the one film used for measuring the length change, additional films separated by filter paper can be inserted. Thus the amount of absorbed gas is increased and it could be detected from the pressure drop in the chamber. Measurements were

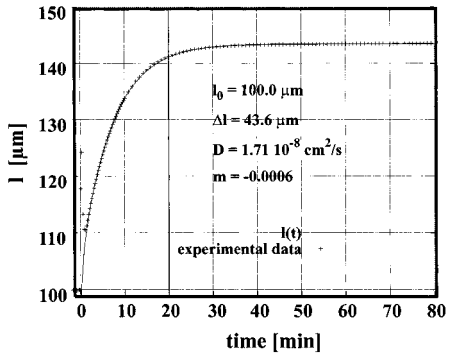

Figure 6. Sample length l (with arbitrary zero point) as a function of time. CO_2 was introduced into the vacuum chamber at $t = 0$ causing a total length change of $\Delta l = 43.6$ μm for TMC-PC. The equation in section 2.3 was fitted to the experimental data points with values of D and m given within the figure.

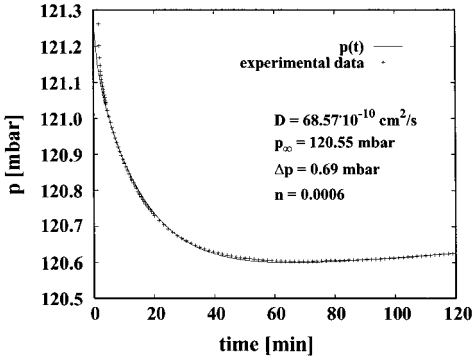

Figure 7. Pressure drop due to sorption as a function of time. Ar was introduced into the vacuum chamber at $t = 0$, causing a total pressure change of $\Delta p = 0.69$ mbar due to sorption by BPA-PC. The equation in section 2.3 was fitted to the experimental data points with given values of D and n.

made the same way as described for the low-pressure dilatometer besides also monitoring the capacitance and pressure changes.

2.3. Time Dependence of *l* and *p*. There is a transient change of pressure and length after changing the gas pressure in the sample chamber. The transient behavior is determined by diffusion of gas molecules into the polymer, as shown for two examples of a measured length and pressure versus time curves presented in Figures 6 and 7. A sum of a linear function and the solution of the corresponding diffusion problem were fitted to the data points. This could be done unambiguously, as the latter describes the rapid changes at the beginning and the linear function determines the long time drift at the end of the experiment. Extrapolating the linear function back to $t = 0$ and subtracting the initial p or l value yields the pressure drop Δp due to gas sorption and the corresponding length change Δl. The solution of the diffusion problem was obtained the usual way[15] from Fick's second law with

initial condition: $c(x,t=0) = 0$

boundary conditions: $c(0,t) = c(d,t) = c_e(p_\infty)$

where c is the concentration of small molecules across the polymer film of thickness d and c_e is the equilibrium concentration from the $p-c$ isotherms for final pressure values p_∞. It has been tacitly assumed that the small changes of the pressure $\Delta p \ll p_\infty$ do not affect the boundary conditions. The solution for the total amount of absorbed gas and the corresponding pressure change (including the drift) has the form

$$p(t) = p_\infty + nt + \sum_{i=1}^{\infty} \frac{8\Delta p}{(2i+1)^2 \pi^2} \exp\left[-\frac{(2i+1)^2 \pi^2 Dt}{d^2}\right]$$

and assuming that the length change is proportional to the amount of absorbed gas yields

$$l(t) = l_0 + mt - \sum_{i=1}^{\infty} \frac{8\Delta l}{(2i+1)^2 \pi^2} \exp\left[-\frac{(2i+1)^2 \pi^2 Dt}{d^2}\right]$$

where n or m is the slope due to the drift and D is an average diffusion coefficient for p in between 0 and p_∞. The diffusion coefficients obtained this way are published elsewhere.[16]

3. Results and Discussion

3.1. CO_2 in Various Polymers. The relative volume changes caused by CO_2 at 294 K in various polycarbonates and Kapton H are plotted in Figure 8 as a function of concentration. The partial molar volume can be defined in two ways (i) as a differential one by the derivative $\partial \Delta V/\partial n$ or (ii) as an integral one by the ratio $\Delta V/n$, where n is the number of moles of dissolved gas. In the following we have used the second definition, which corresponds to the one used in thermodynamics, whereas the first version describes the volume change per additional molecule as used in eq 2. The integral partial molar volume of the absorbed molecule changes from about 2 (Kapton at low concentrations) to 12 cm^3/mol of CO_2 (BPA-PC at high concentrations, cf. Figure 9b). According to Figure 8 the following order with increasing volume change or partial molar volume can be determined: Kapton, TMBPA-PC, TMC-PC, BPZ-PC, and BPA-PC. Within the same order, the volume of the sites occupied by CO_2 molecules should decrease. This decrease can arise from either a lower value of the average site volume V_h° or a lower value of the width σ_V. Polymers with the same average site volume but different widths should lead to different volume changes, because the narrower distribution offers a lower percentage of large sites that are occupied preferentially.

All the results in Figure 8 have in common that the differential partial molar volumes or the slopes increase with increasing concentration. This can be understood in the following way. If sites are smaller than solute molecules, the elastic distortion favors the occupancy of larger sites. At increasing concentration, the smaller sites have to be occupied as well and, therefore, the partial molar volume increases.

A quantitative evaluation starts with eqs 1−6, which were used first to fit $p-c$ isotherms, yielding the two parameters $G°-\mu°$ and σ_G. A detailed description of the fitting procedure is given elsewhere.[9] Then the curves in Figure 8 were calculated with the single fitting parameter V_h° left (V_g for CO_2 is 76.7 Å^3/molecule = 46 cm^3/mol[9]). Table 1 compiles the values of the quantities obtained this way.

If we compare our results in Figure 9a with those of Pope et al.[17] obtained at higher partial pressures of CO_2, there is good agreement with deviations from the predictions of the model occurring for $c > 30$ cm^3/cm^3 or $\Delta V/V > 3\%$. These deviations are more pronounced if we compare the partial molar volumes in Figure 9b, and they are explained as before[9] by swelling of the matrix because the elastic limit has been exceeded. Finally, at the highest concentration the partial molar volume is equivalent with the one in the liquid or rubbery state. This indicates pronounced softening or even a glass/rubbery transition.

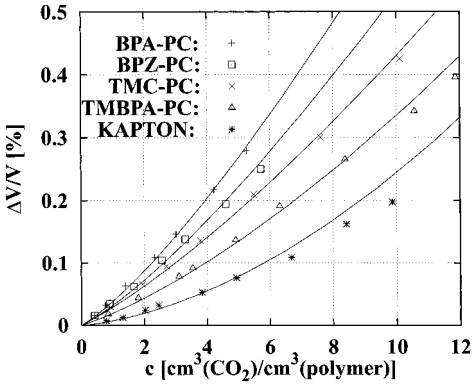

Figure 8. Relative volume expansion as a function of absorbed CO_2 in various glassy polymers at 21 °C. The lines were calculated as described in the text.

Table 1. Some Properties and Fitting Parameter for the Polymers Shown in Figure 1[a]

	polymer				
	BPA-PC	BPZ-PC	TMC-PC	TMBPA-PC	Kapton
T_g (K)	423	458	506	476	693
μ_s (GPa)	0.80	0.86	0.86	0.94	0.9
$G°-\mu°$ (kJ/mol)	15.9	15.4	12.1	12.8	17
σ_G (kJ/mol)	8.9	8.8	7.4	8.4	12.0
$V_h°$ (Å³)	30.7	32.9	36.9	37.5	32.4
σ_V (eq 7) (Å³)	8.0	8.6	9.7	10.5	10.9
σ_V (eq 6) (Å³)	10.9	11.8	13.1	12.8	14.4
r_h (Å) (CO_2)	1.94	1.99	2.06	2.08	1.98
r_h (Å) (e^+)	2.82	2.74	3.15	3.17	
d (Å) (X-rays)	5.08	5.24	5.82	5.86	
$r_h(CO_2)/d$ (X-rays)	0.38	0.38	0.35	0.35	
V_f/V (Bondi)	0.164	0.156	0.190	0.180	

[a] T_g = glass transition temperature (determined by DSC), μ_s = shear modulus (from mechanical spectroscopy[18]), $G°-\mu°$ = average of free energy of solution at 294 K, σ_G = width of G distribution, $V_h°$ = average of the site volume, σ_V = width of V_h distribution calculated from eq 6 with B = 3 GPa or from σ_G via eq 7, r_h = radius calculated for spherical holes obtained from CO_2 sorption or positron annihilation,[18] d = d spacings, V_f/V = fraction of free volume from a group contribution method of Bondi.[19]

3.2. Comparison with Other Values Related to Hole Sizes. With the exception of Kapton the polymers studied in this work form o-positronium during irradiation with positrons.[7] According to a simple model and calibrations with known hole sizes in molecular solids, a relation has been set up[6] between the hole radius r_h and the o-positronium lifetime. Values obtained in this way are included in Table 1. It can be seen that both positron annihilation and CO_2 sorption attribute larger values to TMC-PC and TMPBA-PC when compared to BPA-PC and BPZ-PC. This appears to be reasonable, as the latter have less spacious or more flexible side groups. This is also in agreement with the free volume fraction V_f/V as calculated by a group contribution technique according to Bondi.[19] In addition, the d spacing shows the same separation in the two groups of polycarbonates. However, the ranking among BPA-PC and BPZ-PC is different. CO_2 sorption data agree with d spacings, and positron data agree with free volume fractions.

Although the radii calculated from the models of CO_2 sorption and positronium lifetime differ by only 50%, the corresponding site volumes are different by a factor of 3. The site volume from positron annihilation would be much larger than the volume of the CO_2 molecule and other molecules (see below), and therefore, no volume expansion would be expected during CO_2 sorption, contrary to experimental findings. This discrepancy remains to be resolved by future studies.

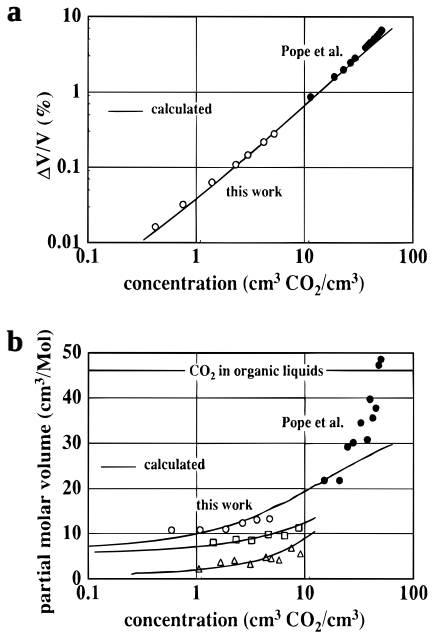

Figure 9. (a) Relative volume change for CO_2 in BPA-PC as a function of concentration: (open circles) own data at 21 °C; (closed circles) Pope et al.[17] at 35 °C. The line was calculated (cf. text). (b) Integral partial molar volume as a function of concentration: (open circles) own data at 21 °C; (closed circles) Pope et al.[17] at 35 °C. In addition, our own data for Kapton-H (triangles) and TMC-PC (squares) at 21 °C are included for comparison. The lines were calculated (cf. text).

If we assume that the d spacing describes the closest distance of adjacent macromolecules, it is equivalent to the diameter of the macromolecular backbone. In the following a simple model is used for relating the site volume to d. Macromolecules are approximated by cylinders and packed in three different ways, as shown in Figure 10. Thus a relationship between the d spacing and the radius of the holes formed in the various structures is obtained. For hexagonal dense packing of parallel cylinders (Figure 10a) the hole radius is $r_h = 0.077d$. This structure represents the crystalline state. Its low solubility of small molecules would be explained in the model of this study by the very small site volume and the concomitant large elastic energy due to eq 1. The square centered arrangement as shown in Figure 10b yields $r_h = 0.20d$, whereas the structure of Figure 10c with stiff cylinders directed in all three dimensions gives $r_h = 0.5d$. The experimental values are shown in Table 1. They can be described by $r_h = (0.365 \pm 0.015)d$. A lower value compared to Figure 10c appears to be reasonable as the coarse woven structure would become denser by using flexible cylinders. We do not want to overestimate the importance of these considerations, but they help to visualize the relationship between the "thickness" of a macromolecule and the size of the interstices.

3.3. Site Energy Parameters and Their Relation to Site Volume. With the values of the average hole volume $V_h°$ we calculated the width of the volume distribution σ_V via eq 7 from experimental values of σ_G. The values are included in Table 1. They are about 30% smaller than the ones calculated from eq 6 with B = 3 GPa (a reasonable value for a liquid polymer at around 500 K[20]). The same discrepancy remains if σ_G is calculated directly from eqs 6 and 7, as shown in Table 2. In light of the approximate nature of the model, the agreement between theoretical and experimental values of σ_G is considered to be good. In addition, the residual free energy of solution $G_r-\mu°$ calculated from eq 7 is

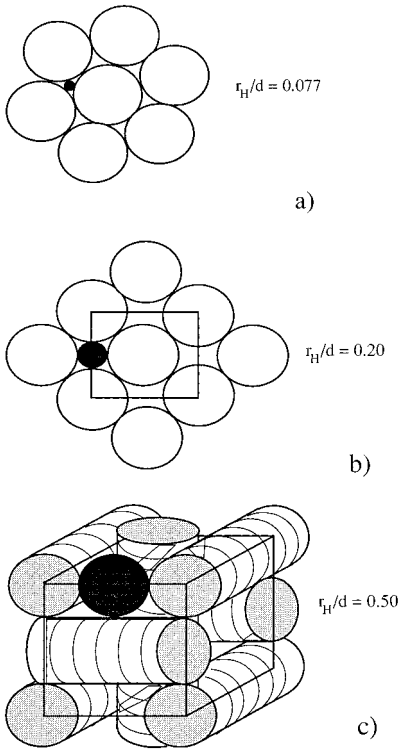

Figure 10. Lattice of cylinders and the related interstitial space (closed circles) for a dense packing of cylinders parallel in one direction (a), square centered and parallel in one direction (b), and three sets of parallel cylinders in all three directions (c). The ratio of the radius r_H of the closed circles and the diameter of the cylinders is included.

Table 2. Calculated Width σ_G-theor of the Gaussian Distribution and the Calculated Residual Free Energy $G_r-\mu°$ (Eq 7)

	polymer				
	BPA-PC	BPZ-PC	TMC-PC	TMBPA-PC	Kapton
$G°-\mu°$ (kJ/mol)	15.9	15.4	12.1	12.8	17
$G_r-\mu°$ (kJ/mol)	1.4	2.3	2.5	2.6	2.6
σ_G-exp (kJ/mol)	8.9	8.8	7.4	8.4	12.0
σ_G-theor (kJ/mol)	12.1	11.8	9.8	10.2	15.8
σ_G-theor/σ_G-exp	1.36	1.34	1.32	1.21	1.32

rather independent of the polymer. This is reasonable, because $G_r-\mu°$ contains contributions from the van der Waals interaction between CO_2 and the rather similar segments of the polymer. Thus, looking at Tables 1 and 2, we can conclude that a large glass transition temperature (Kapton) gives rise to larger values of σ_V and σ_G, leading to smaller volume changes and larger solubilities. The larger site volumes of TMC-PC and TMPBA-PC correspond to smaller elastic energies (cf. eq 1) and, therefore, to higher solubilities (equivalent to lower $G°-\mu°$ values); in addition, the σ_G values are somewhat smaller.

3.4. Various Small Molecules in Polycarbonate BPA-PC. In Figure 11 the volume dilatation caused by acetone in BPA-PC is compared with that of CO_2. In addition, dilatation data for ethylene as taken from ref 21 are included. It is obvious that the volume increase is the larger the larger the size of the molecule. In order to calculate the dilatation, the sorption parameters $G°-\mu°$ and σ_G have to be known. As compiled in Table 3, they were obtained as described previously[9,11] by fitting experimental data (own measurements or ref 21) to eq 5 with a Gaussian function $n(G)$. With these values and the average site volume $V_h^\circ = 30.7$ Å^3 as used for CO_2 sorption, the theoretical curves shown in Figure 11 were calculated. Values for V_g are partial molar volumes in

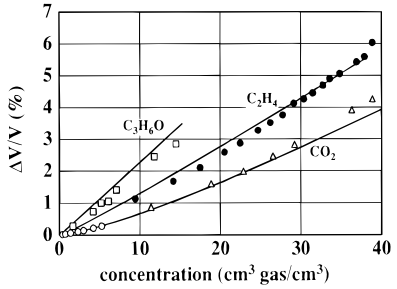

Figure 11. Relative volume change caused by CO_2 [(open circles) own data at 21 °C; (triangles) Pope et al.[17] at 35 °C)], ethylene [(closed circles) from ref 21], and acetone in BPA-PC as a function of concentration. The lines are calculated (cf. text).

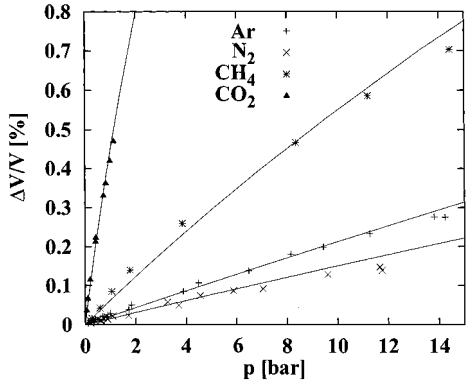

Figure 12. Relative volume change caused by various small molecules in BPA-PC at 21 °C as a function of partial pressure: (▲) CO_2; (*) CH_4; (+) Ar; (×) N_2. The lines are calculated (cf. text).

Table 3. Average Free Energy of Solution $G°-\mu°$ and Width σ_G in BPA-PC As Obtained from Fitting a Gaussian Distribution to Pressure−Concentration Isotherms

	molecule						
	H_2O	Ar	N_2	CH_4	CO_2	C_2H_4	C_3H_{6O}
$G°-\mu°$ (kJ/mol)	0.9	17.2	20.5	18.1	14.9	21.0	6.2
σ_G (kJ/mol)	0	5.1	7.2	7.9	9.3	13	13

the rubbery or liquid state of polymers (CO_2, C_2H_4) or they were calculated from the liquid state of the small molecule (acetone). Thus, no fitting parameter was necessary for ethylene and acetone to obtain the theoretical curves in Figure 11.

For other small molecules besides water, the same procedure was used with the sorption parameters listed in Table 3. However, the partial molar volumes in rubbery polymers taken as V_g differ in these cases. Therefore, we allowed V_g to vary until agreement with experimental dilatation data was achieved. An example is shown in Figure 12, in which $\Delta V/V$ was plotted versus partial pressure in order to separate the data sets more clearly. On $\Delta V/V$ versus c plots, experimental data points are close to each other, as the volumes of the solute molecules do not differ too much. The fitting parameters V_g are compiled in Table 4 and were compared with values obtained from the density of the gas molecules in the liquid state or from dilatation of rubbery polymers. Values of V_g from the liquid state of the small molecules are smaller because they were obtained at low temperatures at least below the boiling point, whereas measurements of volume changes during sorption were made near room temperature. But even in the rubbery state there seemed to be no universal partial molar volume for different polymers. Only CO_2 appears to have constant values independent of the

Table 4. Partial Molar Volumes V_g of the Small Molecules As Measured for the Rubbery or Liquid State of Various Polymers, Molar Volumes of the Same Molecules As Calculated from the Density in the Liquid State of the Solute Molecules and the Values Used for Fitting Measured Volume Changes in the Glassy State[a]

	molecule						
	H_2O	Ar	N_2	CH_4	CO_2	C_2H_4	C_3H_6O
V_g in liquid polymers (Å^3)	30[22]	66.7[24]	66.7−81.7[23,26]	73.3−86.7[23,25]	76.7[23]	95[23]	
V_g in liquid state (Å^3)[27]	30	46.9	57.8	57.2	65		122.5
density (g/cm^3)[27]	1	1.420	0.808	0.466	1.179		0.7899
boiling temp (°C)[27]	100	−189	−196	−164	−57		56.2
V_g used as fitting parameter (Å^3)	30	60.2	68.3	71.7	76.7	95	122.5

[a] The density and the boiling temperature of the small molecules in their liquid state are compiled, too.

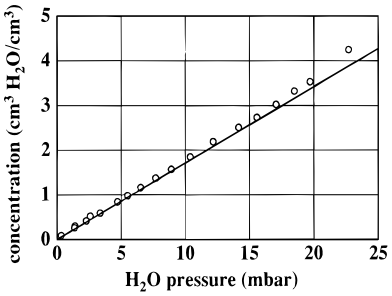

Figure 13. 21 °C isotherm for H_2O in PBA-PC. The straight line is fitted to the low-pressure values and cm^3 H_2O corresponds to the gaseous phase.

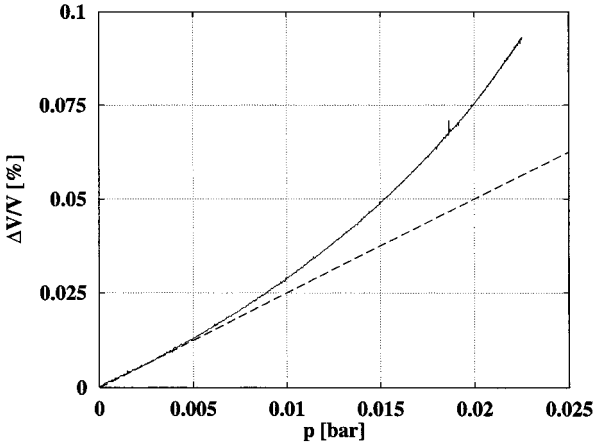

Figure 14. Relative volume change caused by H_2O in a 20 μm thick film of BPA-PC as a function of the partial pressure of water: (solid line) experimental data; (dashed curve) initial linear change. Diffusion was so fast that the length change could be measured continuously.

liquid solvent.[26] Nevertheless, the parameters V_g used to calculate the curves in Figure 12 are in agreement with data from rubbery polymers.

3.5. H_2O in Polycarbonate. In comparison with the solute molecules discussed before, water is different. It is a very small molecule with V_g being slightly smaller than the average site volume (cf. Tables 1 and 4), and it has a permanent dipole, which gives rise to stronger solute−solute interaction and a preferential interaction with dipolar groups of the macromolecules. This may be the reason why the p-c isotherm and the $\Delta V/V$ versus p curves in Figures 13 and 14 look different when compared to Figures 2 and 12.

In agreement with the model of this work, the free energy of dissolution should be independent of V_h, as most of the sites have a larger volume than H_2O. Then the energy distribution function is the Dirac delta function $n(G) = \delta(G - G°)$ and eqs 4 and 5 yield

$$c = p \exp\left[-\frac{G° - \mu°}{kT}\right] \qquad (8)$$

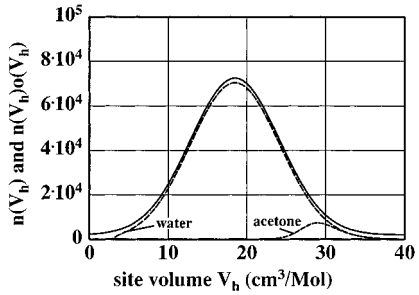

Figure 15. Gaussian distribution of site volumes $n(V_h)$ (solid line, eq 6 with V_h° = 18.5 cm^3/mol and σ_V = 6 cm^3/mol) multiplied with the thermal occupancy $o(V_h) = 1/\{\exp[(G_r + G_{el} - \mu)/kT] + 1\}$ for acetone (dotted line, eq 1 and $G_r - \mu = -25$ kJ/mol) and water (dashed line normalized to the same height as the Gaussian, eq 1 and $G_r - \mu = -25$ kJ/mol). Due to its small volume water molecules occupy most of the sites with equal probability, whereas acetone sits mostly in sites of large volume. Note that the volume change caused by water stems from sites with V_h < 18 cm^3/mol. The Gaussian was shifted upward by 0.2 × 10^4 to avoid coincidence with the dashed line.

i.e., a linear relationship between p and c. This is in agreement with experimental findings at low concentrations, if we use $G° - \mu° = 0.9$ kJ/mol of H_2O (cf. Figure 13). The slight deviations at high concentrations may be attributed to solute−solute interaction, which may be described by a mean field term wc in the chemical potential. A special case of this could be the formation of H_2O pairs, as discussed in more detail below. The straight line shown in Figure 13 can also be obtained with a narrow Gaussian distribution (σ_G < 1 kJ/mol) and $G° - \mu° = 0.9$ kJ/mol of H_2O, which approximates a Dirac delta function.

Although V_g is smaller than many of the sites in BPA-PC, a slight volume dilatation has been observed for water, as seen in Figure 14. Therefore, water molecules occupy smaller holes also, despite the penalty of elastic energy they have to pay and despite the availability of larger holes. This appears to be in contradiction with the model used in this study. However, the calculated elastic energy for water (using eq 1 and parameters from Table 1) is smaller than the thermal energy kT for most of the smaller holes and, therefore, all sites are occupied with equal probability. This different behavior of small molecules when compared to larger ones is also demonstrated quantitatively in Figure 15.

The same formalism for calcualting volume changes may be applied for H_2O, which was previously used for the larger molecules. However, calculating the initial volume change (cf. dashed line in Figure 14), we had to use V_h° = 24.5 Å^3 instead of 30.7 Å^3 in order to describe the behavior at low concentrations. Another possibility would have been to increase the volume of the water molecule from 30 to 36.6 Å^3.

With the small elastic energies involved, the linear expansion of eq 1 used in ref 11 may introduce large errors. In order to avoid this, the assumption of equal occupancy of all sites by H_2O molecules will be applied

for calculating volume changes, too. Then the occupancy is equal to the concentration c and eq 3 will simplify to

$$\Delta V = c \int_0^{V_g} (V_g - V_h) \exp\left[-\frac{(V_h - V_h^\circ)^2}{\sigma_V^2}\right] dV_h \quad (9)$$

where the upper bound of integration is V_g because no volume change occurs for $V_h > V_g$. Equation 9 yields a proportional relation between ΔV and c

$$\Delta V = \frac{c}{2}(V_g - V_h^\circ)\left\{\mathrm{erf}\left[\frac{V_g - V_h^\circ}{\sigma_V}\right] + \mathrm{erf}\frac{V_h^\circ}{\sigma_V}\right\} + \frac{c\sigma_V}{2\sqrt{\pi}}\left\{\exp\left[-\left(\frac{V_g - V_h^\circ}{\sigma_V}\right)^2\right] - \exp\left[-\frac{V_h^{\circ 2}}{\sigma_V^2}\right]\right\} \quad (10)$$

Again, the experimental data at low c (dashed line in Figure 14) can be described only, if we choose either a lower average site volume $V_h^\circ = 24.5$ Å^3 or a larger volume for the water molecule of $V_g = 36.6$ Å^3. We disregard the latter possibility. For the first case one has to take into account that the volume increase caused by water stems from most of the sites having volumes less than V_g. For the larger molecules in Table 4 the elastic energy in small sites becomes larger than the thermal energy and, therefore, only the high volume tail of the Gaussian distribution is occupied. Even for concentrations as large as 40 cm^3 gas/cm^3 polymer c is only 0.16. Thus the average site volume is calculated from data corresponding to a small fraction of sites only. Then the reliability of V_h° depends very sensitively on the real shape of the volume distribution function. Any deviation from a Gaussian yields erroneous average site volumes. Therefore, it is especially helpful to probe the remaining part of the site volume distribution with the very small molecules, in order to obtain more reliable data on the average site volume. This behavior of smaller and larger solutes is demonstrated in Figure 15.

The pronounced upward curvature in Figure 14 is different from the slight downward curvature seen with other small molecules (cf. Figure 12). We propose that this curvature is due to H_2O pair formation. Deviation from the straight line in Figure 13 for the $p-c$ isotherm shall be attributed to pair formation as well. Then at 20 mbar about 0.2 cm^3 H_2O/cm^3 $\approx 10^{-5}$ mol of H_2O/cm^3 form pairs. In order to form a pair an additional H_2O molecule has to be pressed into an occupied site. This gives rise to a volume change of $V_{H_2O} = 18$ cm^3/mol or $\Delta V/V = 1.8 \times 10^{-4}$ (0.018%), in rough agreement with the deviation observed in Figure 14 at 20 mbar with respect to a straight line fitted to the low-pressure results. Therefore, the curvature in Figure 14 can be explained by pair formation. It is much more pronounced than in Figure 13 because the partial molar volume of a pair is so much larger than that of a single solute. Thus H_2O molecules form pairs or clusters at higher concentrations, as observed in polyimides as well.[28]

The reliability of the value for the average site volume V_h° between 25 and 30 Å^3 is now supported by using molecules that differ in their volumes by a factor of 4 and that occupy different parts of the site volume distribution.

3.6. Comparison with Other Methods. The interchain volume and its distribution evaluated from the experimental findings of this work and the model of ref 9 are smaller than that obtained from positron annihilation studies but in between a range of values evaluated from computer simulations.[4,29−31] Reasons for the deviations with respect to positron studies might be the approximations made in deriving the relationship between lifetime and site volume. Neither the model for volume changes by small molecules nor the one for positron annihilation take deviations from a spherical shape of the holes into account, although computer simulations reveal that the holes have irregular shapes.

Acknowledgment. The authors are grateful for financial support provided by the Deutsche Forschungsgemeinschaft.

References and Notes

(1) Shima, R.; Boyer, R. F. *J. Chem. Phys.* **1962**, *37*, 1003.
(2) Struik, L. C. E. *Physical Aging in Amorphous Polymers and Other Materials*, Elsevier, Amsterdam, New York, 1978.
(3) Theodorou, D. N.; Suter, U. W. *Macromolecules* **1986**, *19*, 139.
(4) Greenfield, M. L.; Theodorou, D. N. *Macromolecules* **1993**, *26*, 5461.
(5) Gusev, A. A.; Müller-Plathe, F.; Van Gunsteren, W. F.; Suter, U. W. *Adv. Polym. Sci.* **1994**, *116*, 207.
(6) Jean Y. C.; Deng, Q. *J. Polym. Sci., Polym. Phys.* **1992**, *30*, 1359.
(7) Kluin, J. E.; Yu, Z.; Vleeshouwers, S; McGervey, J. D.; Jamieson, A. M.; Simha, R.; Sommer, K. *Macromolecules* **1993**, *26*, 1853.
(8) Kluin, J. E.; Faupel, F. *Mater. Sci. Forum* **1992**, *105*, 1613.
(9) Kirchheim, R. *J. Polym. Sci., Polym. Phys.* **1993**, *31*, 1373.
(10) Eshelby, J. D. In *Solid State Physics*; Seitz, F., Turnbull, D., Eds.; Academic: New York, 1956.
(11) Kirchheim, R. *Macromolecules* **1992**, *25*, 6952.
(12) Bueche, F. J. *J. Chem. Phys.* **1953**, *21*, 1850.
(13) Grüger, A. Diploma-thesis, University of Göttingen, Germany 1996.
(14) Pott, R.; Schefzyk, R. *J. Phys. E: Sci. Instrum.* **1983**, *16*, 444.
(15) Crank, J. *The mathematics of Diffusion*, 2nd ed.; Claredon Press: Oxford, U.K., 1975.
(16) Pönitsch, M.; Gotthardt, P.; Grüger, A.; Brion, H. G.; Kirchheim, R. *J. Polym. Sci., Polym. Phys.*, in press.
(17) Pope, D. S.; Fleming, G. K.; Koros, W. J. *Macromolecules* **1990**, *23*, 2988.
(18) Sommer, K.; Batoulis, J.; Jilge, W.; Morbitzer, L.; Pittel, B.; Plaetschke, R.; Reuter, K.; Timmermann, R.; Binder, K.; Paul, W.; Gentile, F. T.; Heermann, D. W.; Kremer, K.; Laso, M.; Suter, U. W.; Ludovice, P. J. *Adv. Mater.* **1991**, *3*, 590.
(19) A. Bondi, *J. Phys. Chem.* **1964**, *68*, 441.
(20) Van Krevelen, D. W.; Hoftyzer, P. J. *Properties of Polymers*, 2nd ed.; Elsevier: New York, 1980; Chapter 4.
(21) Barbari, T. A.; Conforti, R. M. *J. Polym. Sci., Polym. Phys.* **1992**, *30*, 1261.
(22) Adamson, M. J. *J. Mater. Sci.* **1980**, *15*, 1736.
(23) Pope, D. S.; Sanchez, I. C.; Koros, W. J.; Fleming, G. K. *Macromolecules* **1991**, *24*, 1779.
(24) Kamiya, Y.; Mizoguchi, K.; Naito, Y.; Bourbon, D. *J. Polym. Sci., Polym. Phys.* **1991**, *29*, 225.
(25) Kamiya, Y.; Terada, K.; Mizoguchi, K.; Naito, Y. *Macromolecules* **1992**, *25*, 4321.
(26) Kamiya, Y.; Naito, Y.; Bourbon, D. *J. Polym. Sci., Polym. Phys.* **1994**, *32*, 281.
(27) *CRC Handbook of Chemistry and Physics*, 59th ed.; CRC Press Inc.: West Palm Beach, FL, 1979.
(28) Lim, B. S.; Nowick, A. S.; Lee, Kang-Wook; Viehbeck, A. *J. Polym. Sci., Polym. Phys.* **1993**, *31*, 545.
(29) Shaw, V. M.; Stern, S. A.; Ludovice, P. J. *Macromolecules* **1989**, *22*, 4460.
(30) Arizzi, S.; Mott, P. H.; Sutter, U. W. *J. Polym. Sci., Polym. Phys.* **1992**, *30*, 415.
(31) Misra, S.; Mattice, W. L. *Macromolecules* **1993**, *26*, 7274.

MA9708252